OBSERVATION AND ANALYSIS OF LEATHER STRUCTURE BASED ON NANO-CT

Huayong Zhang[1, b], Jinyong Cheng[2], Tianduo Li[2, a], Jianmei Lu[2], Yuai Hua[2]

1 State Key Laboratory of Biobased Material and Green Papermaking, Qilu University of Technology (Shandong Academy of Sciences), Jinan, 250353

2 Shandong Provincial Key Laboratory of Fine Chemicals, Qilu University of Technology (Shandong Academy of Sciences), Jinan, 250353

a) Corresponding author: ylpt6296@vip.163.com

b) headingzhy@126.com

Abstract. The composition, working principle and the image acquisition procedure of nano-CT were introduced. A dried piece of blue stock of chrome-tanned cattle hide was chosen for this work and a sequence of 2357 images was obtained. 3D visible digital models of leather fiber bundle braided network and the interspace between fiber bundles were reconstructed. The inner structure and composition of leather were shown accurately and intuitively in the form of 2D sectional images and 3D image. Based on the 3D model, the diameter, volume, surface area and other parameters of the fiber bundles, the pore structure and inclusions were measured and calculated.

1 Introduction

Leather is formed by tight weaving of collagen fiber bundles. The three-dimensional (3D) weaving network of collagen fibers is the structural basis of physical and mechanical properties of leather. Recognizing and studying this three-dimensional weaving network of collagen fibers can facilitate researches on structure-performance relationship of leathers effectively and promote improvement and development of leather production techniques[1]. There are many methods to acquire the 3D weaving structure of leather, including microtomy, layered polishing method of metallographic preparation sample, magnetic resonance imaging (MRI) imaging method and micro-CT method[2-5]. Among them, the first two methods are time and labor-consuming ones. Although MRI imaging method won't cause damages to samples, it has low resolution and high cost. In this study, micro-CT method which causes no damages to samples and has high resolution was applied.

CT is the short for computed tomography. Micro-CT generally refers to CT with the spatial resolution reaching l μm~10 μm. It is a non-invasive and non-destructive imaging technique and scans samples by X-ray to acquire internal structural information of samples, without damaging samples[6]. Later, it composes the 3D structural images of samples based on analysis and processing, thus getting thorough three-dimensional structural information of samples. Micro-CT is widely applied in many research fields, such as medicine, materials, biology, archaeology, electronic engineering and geology [7-10].

The small size of leather fiber bundles and complicated weaving structure proposed high requirements on performance and parameter setting of instruments. So far, there are few studies on three-dimensional structure of leather based on micro-CT. In 2014, E.Bittrich et al. studied structure of leather by micro-CT and acquired the 3D structure of vegetable tanned leather under the resolution of 3.3μm. However, they failed to get clear structure images of chrome tanned leather, which were attributed to influences of tanned metals[5].

In this study, scanning steps and imaging observation method of high-resolution micro-CT to chrome tanned leather were explored and introduced systematically. Research conclusions can provide certain assistances and references to further study 3D structure of leather.

2 Experimental Materials and Instruments

Dried pieces of blue stock of chrome-tanned cattle hide provided by Qilu university of technology leather laboratory was chosen for this work.

The micro-CT Equipped with CCD detector and analysis software was Bruker SkyScan2211, Belgium.

3 Experimental methods

3.1 Composition and principle of micro-CT

The major component of micro-CT is composed of X-ray source, rotating sample platform and high-resolution detector (Fig. 1). In addition, it covers the control system and computer processor, etc. Structure of micro-CT is shown in Fig. 1.

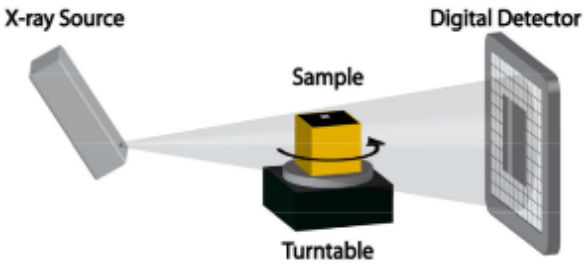

Fig. 1. Schematic diagram of micro-CT system.

X-ray emission source and detector were fixed, while samples rotated between X-ray source and detector. Besides, samples could move vertically and horizontally. The conical X-ray bundles which are produced continuously by X-ray source penetrate samples and images of the sample was produced on the X-ray detector. Since the penetrability of X-ray in different substances is difference, light intensity at different positions of the detector varies. According to light intensity produced gray image[11], projection image of sample from this perspective is acquired. The X-ray projection images of the sample from different perspectives are gained by rotating it at a certain angular rate. After series of projection images are acquired, data of these projection images were processed by certain mathematical algorithm, thus getting three-dimensional information of the sample. Processing and analysis of data formed by micro-CT scanning requires the use of special three-dimensional analysis software.

3.2. 2D images Acquisition by micro-CT

3.2.1 Determination of scanning parameters

In this experiment, resolution was set 1.5μm/pixel and the leather sample size was about 5.4mm×3.5mm×3.9mm. According to structural properties of leather, image qualities under different parameters were observed and compared. With comprehensive consideration to efficiency and quality, CCD detector was chosen. Scanning parameters were set: Voltage and current of the light tube were 50KV and 320μA, respectively. The exposure time was 1000ms and the focusing current was 620.9mA. The scanning step length was 0.2° and each step had 8 scans. The scanning angle was 180°. The scan took a total of 3h and 38 minutes, getting 970 projection images. The image pixel size was 4032×2688 (bmp format, 10.3M). Four images are shown in Fig. 2. Since projection image was gained after ray penetrating through the whole sample, it superposed multiple layers of sample information and couldn't reflect the leather structure intuitively.

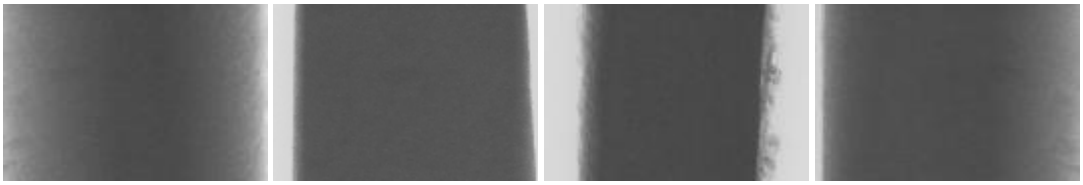

Fig. 2. Leather projection images acquired by micro-CT.

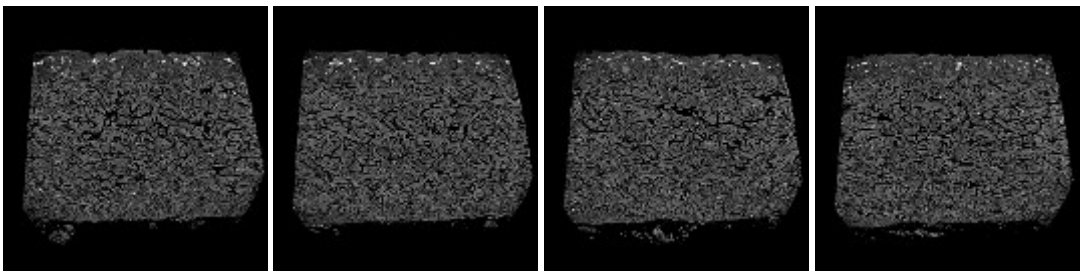

Fig. 3. Leather section images reconstructed from the series CT projection images.

3.2.2 Reconstruction and observation of 2D section images

Section images of leather were reconstructed from the series projection images by the NRecon software. Firstly, the series projection images were aligned and eliminated negative influences of ring artifact and beam hardening, accompanied with appropriate smoothing. Next, 2D sections were reconstructed and 2357 series images of 2D section (x-y) were produced. Pixel size of each section image was 4032×4032(bmp format, 15.5M) and the interlayer distance was 1 pixel (1.5μm). Four section images are shown in Fig.3. It can be seen from Fig.3 that the grain surface and reticular layer of this leather sample were distinguished obviously.In the grain layer, fiber bundles are thin and weaved tightly. In the reticular layer, fiber bundles of the middle portion are thick and weaved loosely, showing big spaces between fiber bundles. Some fiber bundles close to the grain layer and meat layer are thin and weaved slightly tightly. Many white bright spots in Fig.3 are high-density crystals which are not processed cleanly. There are many large white bright spots in the grain layer, but there are few small spots on the reticular layer.

Three orthogonal section images centered at any point of the reconstructed space were displayed by the DataViewer software. Pixels were expressed in different colors according to the gray value. For example, in Fig.4, three orthogonal section images which passed through one point were clear. The same structure could be observed from different perspectives to reflect fiber bundles and pores intuitively. In addition, all structures can maintain the original shape completely by using the digital slicing method, without deformation and falling.

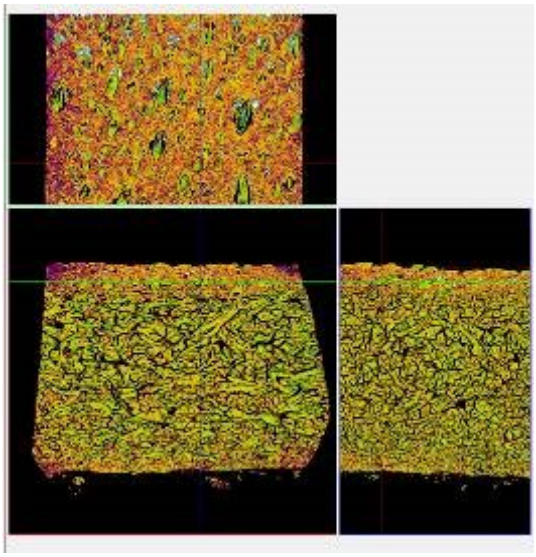

Fig. 4. Three orthogonal section images of leather.

3.2.3 Reconstruction, observation and measuring quantitative parameters of 3D images

Series 2D section images were reconstructed into 3D images by the volume rendering software CTVOX. By setting transparency of pixel points with different gray values and certain color the three-dimensional structure of overall structure or one substructure was reflected intuitively (Fig.5a). When the fiber bundles and pores were set transparency, 3D distribution of high-density crystals was observed (Fig.5b). Moreover, random digital cutting could be carried out and one part of the result was displayed and processed. For example, the 3D digital model of the selected part position was shown in Fig.6. Obviously, the part surface of grain layer was cut off, which exposed the pores or veins clearly (Fig.6a). The high-density white crystals were exposed (Fig.6b).

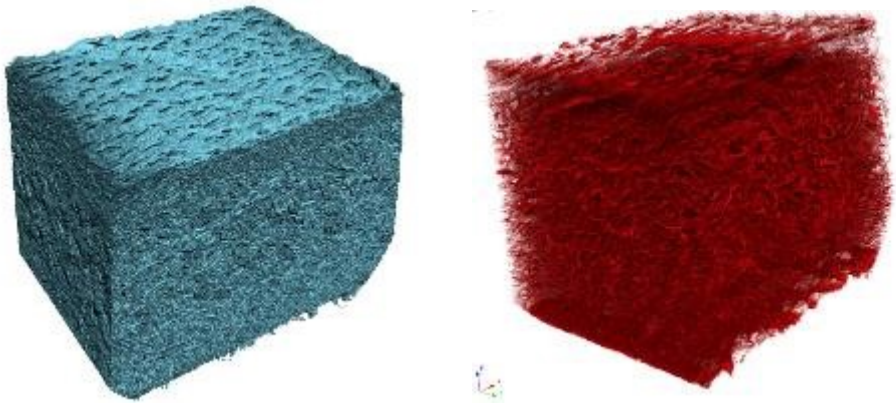

(a) leather fiber bundle braided network (b) interspace between fiber bundles

Fig. 5 3D volume rendering reconstruction images of leather (5.4mm×3.5mm×3.9mm).

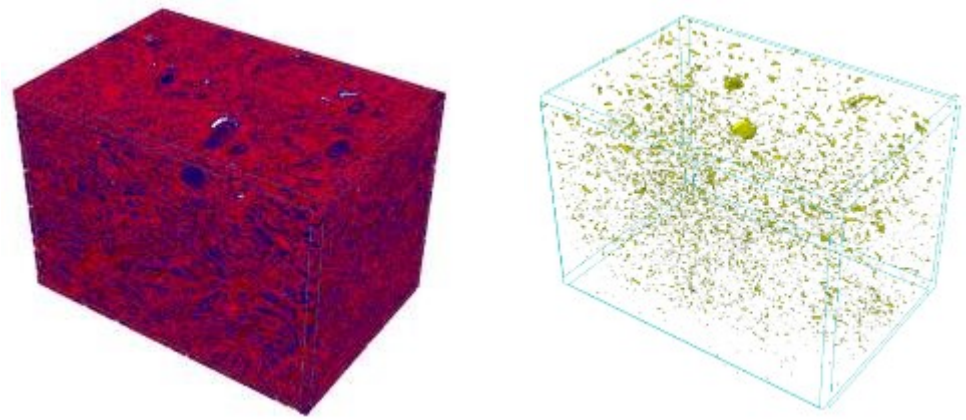

(a) (b)

Fig.6 Selected part position of 3D digital model (3mm×1.5mm×2mm).

Based on the 3D model, the diameter, volume, surface area and other parameters of the fiber bundles, the pore structure and inclusions were measured and calculated by CT-analyser software. Partial 3D analysis based on the 3D model of Fig. 5a see Table 1, and the structure thickness (Diameter of fiber bundles) distribution see Table 2.

Table 1. 3D analysis of the 3D model.

Description	Value	Unit
Total VOI volume	70239387385	um^3
Object volume	46193939033	um^3
Percent object volume	65.77	%
Total VOI surface	152146821	um^2
Object surface	4053470740	um^2
Intersection surface	53355506	um^2
Object surface / volume ratio	0.08775	1/um
Object surface density	0.05771	1/um
Number of objects	14027	
Number of closed pores	361841	
Volume of closed pores	504048841	um^3
Surface of closed pores	214219493	um^2
Closed porosity (percent)	1.08	%
Volume of open pore space	23541399511	um^3
Open porosity (percent)	33.52	%
Total volume of pore space	24045448352	um^3
Total porosity (percent)	34.60	%

4 Conclusions

A method to acquire and observe 3D weaving structure of leather through micro-CT was introduced. The composition and principle, parameter settings and data acquisition steps of micro-CT were introduced thoroughly. Images were processed by corresponding software accordingly, thus getting the series 2D and 3D images of chrome-tanned leather. The gained 3D digital structure has following purposes and significance: it is not only beneficial to further study the morphology of 3D structure

of leather accurately and thoroughly, but also to explore the relationship between structure and performance of leather. Assisted by corresponding image processing tool, any slices or internal structure of 3D volume can be analyzed deeply through a series of cutting, enhancing and measurement functions, such as measuring morphological parameters of leather fiber bundles and pores (e.g. diameter, length, specific surface and volume), studying distribution pattern of fiber bundles, observing connectivity of spaces among fiber bundles, and calculating physical parameters (e.g. porosity, volume density and fractal dimension) of leather. Further studies on these aspects will be carried out in future.

Table 2. Structure thickness distribution.

Range	Mid-range	Volume	Percent volume in range
um	um	um^3	%
1.50 - 4.50	3	22374160.5	0.0485
4.50 - 7.50	6	201329951.5	0.4361
7.50 - 10.50	9	345494838.7	0.7484
10.50 - 13.50	12	968296506.9	2.0974
13.50 - 16.50	15	1683379913	3.6463
16.50 - 19.50	18	2090130837	4.5274
19.50 - 22.50	21	3156601127	6.8374
22.50 - 25.50	24	3430937981	7.4317
25.50 - 28.50	27	3561692161	7.7149
28.50 - 31.50	30	3707121253	8.0299
31.50 - 34.50	33	3814585777	8.2627
34.50 - 37.50	36	3273281346	7.0902
37.50 - 40.50	39	3271279391	7.0858
40.50 - 43.50	42	2982358271	6.46
43.50 - 46.50	45	2425641873	5.2541
46.50 - 49.50	48	2146793315	4.6501
49.50 - 52.50	51	1925423249	4.1706
52.50 - 55.50	54	1562657940	3.3848
55.50 - 58.50	57	1307396731	2.8319
58.50 - 61.50	60	1020285284	2.21
61.50 - 64.50	63	807400344.4	1.7489
64.50 - 67.50	66	635641526.3	1.3768
67.50 - 70.50	69	474858622.4	1.0286
70.50 - 73.50	72	362268497.3	0.7847
73.50 - 76.50	75	258186644.4	0.5593
76.50 - 79.50	78	194791460	0.4219
79.50 - 82.50	81	144638910.8	0.3133
82.50 - 85.50	84	109573726.7	0.2373
85.50 - 88.50	87	77387817.79	0.1676
88.50 - 91.50	90	56490527.97	0.1224
91.50 - 94.50	93	38037136.99	0.0824
94.50 - 97.50	96	28998738.37	0.0628
97.50 - 100.50	99	16561532.43	0.0359
100.50 - 103.50	102	13055085.92	0.0283
103.50 - 106.50	105	11628597.39	0.0252

Acknowledgements

This work was supported by the Project of Natural Science Foundation of Shandong Province (No. ZR2017LB024), the National Natural Science Funds of China (No. 211776143), and Program for Li Tianduo Taishan Scholar Team of Shandong Province.

References

1. *Yuan, J.J., Leather Sci. and Eng. 21, 19-21, 2011*
2. *Luo, L. S., Materials Rev. 24(09), 1-5, 2010.*
3. *Zhang, H. Y., J. Amer. Leather Chem. Ass., 2014, 109, 1.*
4. *Zhang, H. Y., J. Amer. Leather Chem. Ass., 2018, 113,248*
5. *Zhang, H. Y., J. Soc. Leather Technol. Chem., 2015, 99, 23.*
6. *Bittrich E. J. Amer. Leather Chem. Ass., 2014,109,367*
7. *Moreno-Atanasio R, Particuology, 2010 (8): 81*
8. *Kariem H, J Materials Sci., 2018:1.*
9. *Zhou M, Energies, 2018, 11(6):1409.*
10. *Heyndrickx M, Mater Charact. 2018, 139:259.*
11. *Zauer M , Wood Sci. Technol, 2014, 48(6):1229.*
12. *Sukop M C, Phys. Rev. E, 2008, 77: 026710.*